

Enhancing Robustness of Implicit Neural Representations Against Weight Perturbations

Wenyong Zhou*

Department of EEE

The University of Hong Kong
Hong Kong SAR

Yuxin Cheng*

Department of EEE

The University of Hong Kong
Hong Kong SAR

Zhengwu Liu†

Department of EEE

The University of Hong Kong
Hong Kong SAR

Taiqiang Wu
Department of EEE
The University of Hong Kong
Hong Kong SAR

Chen Zhang
Department of EEE
The University of Hong Kong
Hong Kong SAR

Ngai Wong†
Department of EEE
The University of Hong Kong
Hong Kong SAR

Abstract—Implicit Neural Representations (INRs) encode discrete signals in a continuous manner using neural networks, demonstrating significant value across various multimedia applications. However, the vulnerability of INRs presents a critical challenge for their real-world deployments, as the network weights might be subjected to unavoidable perturbations. In this work, we investigate the robustness of INRs for the first time and find that even minor perturbations can lead to substantial performance degradation in the quality of signal reconstruction. To mitigate this issue, we formulate the robustness problem in INRs by minimizing the difference between loss with and without weight perturbations. Furthermore, we derive a novel robust loss function to regulate the gradient of the reconstruction loss with respect to weights, thereby enhancing the robustness. Extensive experiments on reconstruction tasks across multiple modalities demonstrate that our method achieves up to a 7.5 dB improvement in peak signal-to-noise ratio (PSNR) values compared to original INRs under noisy conditions.

Index Terms—Implicit Neural Representations, Reconstruction Robustness, Weight Perturbation

I. INTRODUCTION

Implicit Neural Representations (INRs) provide a flexible approach to encoding various signals, including images, audio, and video [1]–[4]. INRs model signals as continuous functions parameterized by neural networks, typically implementing Multi-Layer Perceptrons (MLPs) [5]. For example, when modeling a two-dimensional grayscale image, INRs map pixel coordinates to their corresponding grayscale values, enabling high-quality signal reconstruction while supporting signal interpolation and super-resolution. Due to these capabilities, INRs have gained significant traction in various applications [6]–[8].

Previous works have primarily focused on improving the performance and efficiency of INRs. Various complex activation functions, including sinusoidal, Gaussian, and wavelet

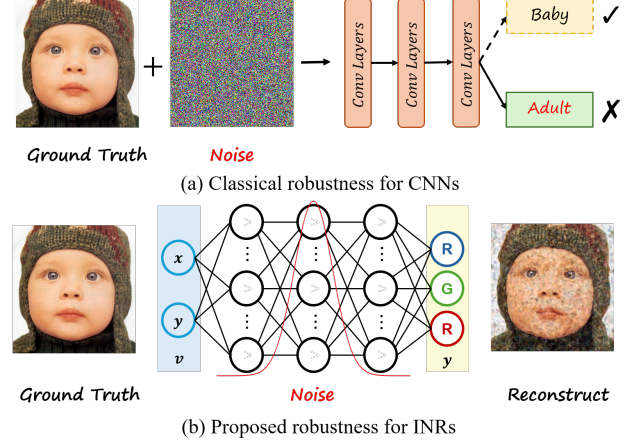


Fig. 1. Comparison of robustness between classical CNNs and INRs: (a) In classical CNNs, noise typically corrupts input images, leading to misclassification or errors in the task. (b) In INRs, noise perturbs the model weights, resulting in degraded reconstruction performance.

functions, have been explored to enhance the high-frequency representation capabilities of neural networks in INRs, enabling them to capture finer signal details [9]. To accelerate the training process, [10] proposed a simple random permutation of pixel locations, while [11] introduced an efficient data sampling framework by formulating INR training as a nonparametric teaching problem. However, a critical challenge overlooked by existing work is the robustness of INRs.

The robustness challenge in INRs is fundamentally distinct from that in Convolutional Neural Networks (CNNs). In CNNs, robustness primarily targets resistance to adversarial samples that subtly perturb input images with minimal content changes, as depicted in Figure 1 [12]–[15]. In contrast, INR robustness concerns shift from input data to model weights, as the signal is encoded directly in the network parameters. Sources of weight perturbations include model transmission errors, compression inaccuracies, and hardware constraints in devices like compute-in-memory (CIM) systems [16]–[19]. Even minimal perturbations can significantly impair INR per-

*: Equal contributions. †: Corresponding authors: Zhengwu Liu and Ngai Wong {zwliu, nwong@eee.hku.hk}. This work was supported in part by the Theme-based Research Scheme (TRS) project T45-701/22-R, National Natural Science Foundation of China (62404187) and the General Research Fund (GRF) Project 17203224, of the Research Grants Council (RGC), Hong Kong SAR.

formance due to the sensitivity of reconstruction tasks [8], [20]. Furthermore, traditional robustness-enhancing methods like adversarial training and data augmentation are less effective for INRs [21], [22]. Adversarial training typically generates perturbed input samples to improve model robustness, but in INRs, the input coordinates remain fixed and unperturbed since they serve as query points for signal reconstruction. Data augmentation methods that modify input data (e.g., rotation, scaling, or adding noise) do not align with the INR paradigm, where the challenge lies in weight perturbations rather than input variations.

To address this challenge, we present the first systematic investigation of INR vulnerability to weight perturbations and propose a robust loss function to enhance model resilience. Our main contributions are threefold:

- We present a systematic investigation of the robustness of INRs under weight perturbation and find that even a tiny perturbation can lead to significant degradation in reconstruction quality.
- We formulate the robustness problem in the INR context by minimizing the reconstruction distance between clean and perturbed weights. Based on the formulation, we derive a novel robust loss function to enhance the robustness of INR.
- Extensive experiments on reconstruction tasks across multiple modalities demonstrate that our method yields improvements of up to 2.5 dB in PSNR values compared to the baseline INR under various noise conditions.

II. METHODOLOGY

This section begins by demonstrating the vulnerability of INRs in the image reconstruction task. To address this issue, we formulate the problem and propose a gradient-based loss function to regularize the gradient of the reconstruction loss with respect to the model weights.

A. Vulnerability of INRs for Reconstruction Tasks

Given the differences in robustness between CNNs and INRs, we first explore the impact of weight perturbations on INRs in the image reconstruction task, as visualized in Figure 2. In the figure, the left column shows the original images reconstructed by the INR model without any noise. These images are clear and retain the original details, demonstrating the model's ability to accurately capture and represent the input data. The middle and right columns introduce Gaussian and binary noise into the model weights, resulting in a noticeable decline in image quality. While the images still maintain basic structure, the added noise causes significant blurring and distortion, underscoring the model's limited robustness to weight perturbations. It should be noted that the noise applied was only 1% of the true value of the model weights, or only 1% of the parameters were masked to zero. While this typically results in negligible performance degradation in classification tasks for CNNs, it leads to severe degradation in INRs.

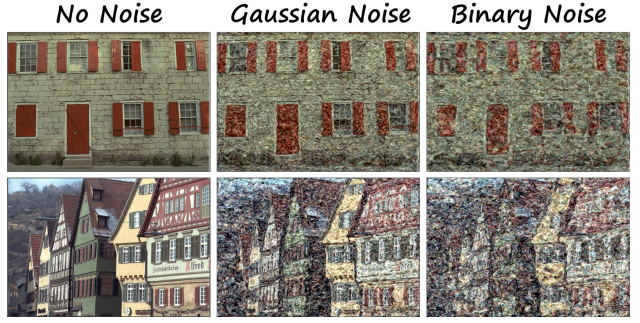


Fig. 2. The reconstruction of INRs with and without weight perturbations on Kodak01, Kodak08 images under Gaussian and binary noises.

B. Gradient-Based Loss for Improving INR Robustness

The previous section demonstrates the difference in noise impact on classical CNNs and INRs. To obtain a better understanding, we formulate the robustness problem in this subsection and then propose our gradient-based loss function.

Suppose the continuous signal that we want to reconstruct is a function $f : \mathbb{R}^n \rightarrow \mathbb{R}^m$, where n is the dimensionality of the input space (e.g., coordinates for an image) and m is the dimensionality of the output space (e.g., 3 for RGB values). The INR model \hat{f}_θ is a MLP parameterized by θ , which approximates f . Given a set of discrete samples $\{(\mathbf{x}_i, \mathbf{y}_i)\}_{i=1}^N$, where $\mathbf{x}_i \in \mathbb{R}^n$ are the input coordinates and $\mathbf{y}_i = f(\mathbf{x}_i)$ are the corresponding output values, the goal of the INR model is to learn the parameters θ to minimize the reconstruction loss:

$$\mathcal{L}(\theta) = \frac{1}{N} \sum_{i=1}^N \left\| \hat{f}_\theta(\mathbf{x}_i) - \mathbf{y}_i \right\|_2^2 \quad (1)$$

When model weights θ are perturbed by some slight noise $\Delta\theta$, the new set of parameters $\theta + \Delta\theta$ will create a new image whose reconstruction loss is:

$$\mathcal{L}(\theta + \Delta\theta) = \frac{1}{N} \sum_{i=1}^N \left\| \hat{f}_{\theta+\Delta\theta}(\mathbf{x}_i) - \mathbf{y}_i \right\|_2^2 \quad (2)$$

Although minimizing Eq. 2 yields the best reconstruction results, the presence of unknown noise makes it impossible to directly optimize the reconstruction loss under noisy conditions. Therefore, optimizing a proxy for the noisy reconstruction loss can help guide the model towards a more robust state. Since we want the model's output under noise to be as close as possible to the output in the absence of noise, minimizing the difference between the noisy reconstruction loss and the original reconstruction loss could serve as an effective proxy target. In other words, we aim to achieve $\mathcal{L}(\theta + \Delta\theta) \approx \mathcal{L}(\theta)$, or more precisely:

$$\min_{\theta} \left\| \mathcal{L}(\theta + \Delta\theta) - \mathcal{L}(\theta) \right\| \quad (3)$$

Since the noise $\Delta\theta$ is a small perturbation around the parameters θ , it is possible for us to perform a first-order Taylor expansion around θ , which is given by:

$$\mathcal{L}(\theta + \Delta\theta) = \mathcal{L}(\theta) + \nabla_{\theta} \mathcal{L}(\theta) \cdot \Delta\theta + o(\Delta\theta) \quad (4)$$

where $\nabla_\theta \mathcal{L}(\theta)$ is the gradient of the loss function with respect to θ , and $o(||\Delta\theta||)$ represents higher-order terms that are of smaller order compared to $\Delta\theta$. Omitting the higher-order terms, we could get:

$$||\mathcal{L}(\theta + \Delta\theta) - \mathcal{L}(\theta)|| \approx ||\nabla_\theta \mathcal{L}(\theta) \cdot \Delta\theta|| \leq ||\nabla_\theta \mathcal{L}(\theta)|| \cdot ||\Delta\theta|| \quad (5)$$

Since the noise $\Delta\theta$ is unknown and small, it is important to regularize the gradient term $\nabla_\theta \mathcal{L}(\theta)$ to minimize the difference between the noisy reconstruction loss and the original reconstruction loss. Therefore, we introduce a gradient-based robust loss function $\mathcal{L}_{\text{robust}}(\theta)$:

$$\mathcal{L}_{\text{robust}}(\theta) = \mathcal{L}(\theta) + \lambda \cdot ||\nabla_\theta \mathcal{L}(\theta)|| \quad (6)$$

where λ is a hyperparameter that controls the trade-off between the original loss and the robustness penalty.

During the backpropagation, the gradient of the norm of gradients with respect to θ is derived as:

$$\nabla_\theta ||\nabla_\theta \mathcal{L}(\theta)|| = \nabla_\theta \sqrt{\sum_{i=1}^d \left(\frac{\partial \mathcal{L}}{\partial \theta_i} \right)^2} \quad (7)$$

$$= \nabla_\theta \sqrt{\nabla_\theta \mathcal{L}(\theta) \cdot \nabla_\theta \mathcal{L}(\theta)} \quad (8)$$

$$= \frac{\nabla_\theta \mathcal{L}(\theta)}{||\nabla_\theta \mathcal{L}(\theta)||} \quad (9)$$

The equation shows that the gradient of the norm is the original gradient vector scaled by the reciprocal of its norm. This computation only involves first-order derivatives of $\mathcal{L}(\theta)$, which are typically computed during backpropagation, making it efficient.

III. EXPERIMENTS

In this section, we compare our gradient-based robust loss function with previously proposed robust loss functions on signal reconstruction tasks across multiple modalities to demonstrate the effectiveness of our method.

A. Experiment Setup

Given the novel focus of our study, comparable methods within our specific domain are scarce. Consequently, we have adapted two established loss functions from CNN robustness studies for comparison: the L_1 loss [23] and the Lipschitz loss [24]. Additionally, we include a comparison with noise-aware training [25], which involves injecting noise into the weights during training to simulate realistic noise conditions. All experiments are conducted on a single NVIDIA RTX 3090 GPU.

B. Experiment Results

Main results. We take images from the Kodak dataset as reconstruction images in this experiment and set $\sigma = 1e^{-3}$ for the Gaussian noise condition and $p = 1e^{-3}$ for binary noise. The result is shown in Table I. For Gaussian noise, our method outperforms the other methods by yielding improvements in PSNR values by up to 2.53 dB, 3.01 dB, and 2.16 dB on different images, respectively. Under binary noise, our method

TABLE I
COMPARISON BETWEEN OUR METHOD AND OTHER ROBUSTNESS METHODS WHEN RECONSTRUCTING IMAGES IN THE KODAK DATASET UNDER VARIOUS NOISES.

Methods	PSNR (dB)		
	Kodak01	Kodak08	Kodak24
<i>Gaussian Noise ($\sigma = 0.001$)</i>			
MSE Loss	15.73	12.42	14.96
+ L_1 Loss [23]	15.41	11.88	14.88
+ Lipschitz Loss [24]	15.11	11.47	14.55
+ Noise-aware Training [25]	15.26	11.57	14.62
Ours	17.64	14.48	16.71
<i>Binary Noise ($p = 0.001$)</i>			
MSE Loss	18.57	13.48	17.29
+ L_1 Loss [23]	18.70	13.51	17.32
+ Lipschitz Loss [24]	18.41	13.60	17.49
+ Noise-aware Training [25]	17.32	13.50	17.08
Ours	22.48	16.36	22.38

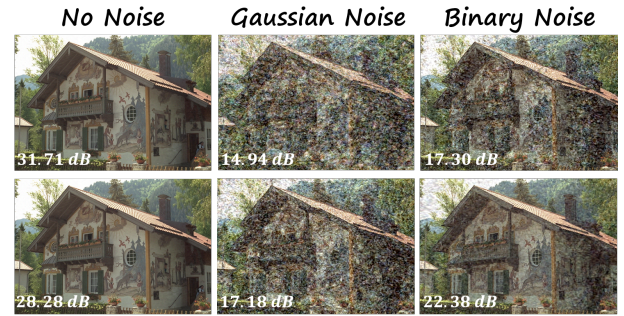


Fig. 3. The reconstruction results between baseline SIREN (first row) and our method (second row) under noise-free, Gaussian noise and binary noise condition on Kodak24 images.

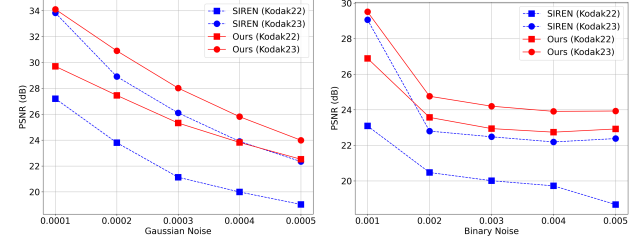


Fig. 4. Comparison of baseline SIREN and our method on Kodak22 and Kodak23 images reconstruction under various Gaussian and binary noise conditions.

again shows consistent superior performance by improving the PSNR values by up to 5.16 dB, 2.88 dB, and 5.30 dB for different images, respectively.

Figure 3 compares the reconstruction results of the vanilla model and our method. It can be seen that our method preserves more details under both Gaussian and binary noise. Moreover, we test different noise strengths of both types and report the PSNR in Figure 4. Although there is performance degradation in noise-free conditions, our method demonstrates consistently superior performance compared to the vanilla model.

More modality results. To demonstrate the generalization

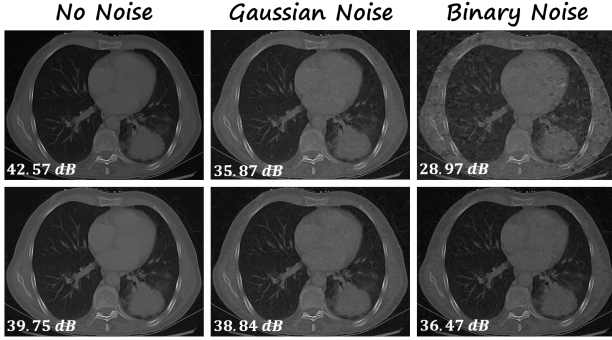


Fig. 5. Reconstruction comparison of baseline SIREN (first row) and our method (second row) for CT image reconstruction under Gaussian and binary noise conditions.

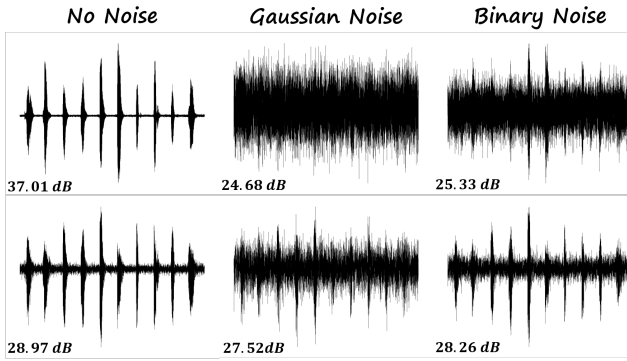


Fig. 6. Comparison of baseline SIREN (first row) and our method (second row) for audio signal reconstruction under Gaussian and binary noise conditions.



Fig. 7. Comparison of baseline SIREN (left two columns) and our method (right two columns) for video signal reconstruction under Gaussian and binary noise conditions.

capability of our proposed method, we conduct more experiments across multiple modalities, including medical computed tomography (CT) image in Figure 5, audio in Figure 6 and video in Figure 7 [26], [27]. In Figure 5, the baseline SIREN

TABLE II
ABLATION STUDY ON THE HYPERPARAMETER OF λ ON Kodak IMAGES UNDER GAUSSIAN NOISE ($\sigma = 0.001$).

Value of λ	PSNR (dB)			
	Kodak01	Kodak08	Kodak12	Kodak24
$\lambda = 0.01$	16.20	13.42	19.89	15.24
$\lambda = 0.1$	17.64	14.48	19.61	16.63
$\lambda = 0.2$	17.61	14.43	20.21	16.53
$\lambda = 0.5$	18.17	14.05	19.34	16.71

outperforms our approach by 2.82 dB in the absence of noise, but our method are more robust under noise conditions by yielding up to a 7.5 dB in PSNR value. For audio signal reconstruction, a similar trend can also be observed: the reconstruction of our method is 8.04 dB lower than that of the vanilla SIREN model but achieves a PSNR increase of up to 2.84 dB under Gaussian noise and 2.93 dB under binary noise. For video reconstruction, as shown in Figure 7, we conduct an experiment on a 2-second video with 25 frames per second. As expected, our method excels in noisy environments, delivering a PSNR increase of up to 0.26 dB under Gaussian noise and 1.74 dB under binary noise. All the above experiments demonstrate that our method can effectively enhance the robustness of INRs in various applications.

C. Ablation Study

The ablation study presented in Table II examines the impact of varying the regularization hyperparameter λ on the performance of our method, as measured by PSNR across four Kodak images, which is the same as those in Table I for consistency under Gaussian noise ($\sigma = 1e^{-3}$). The results demonstrate that reconstruction quality is highly dependent on the choice of λ . Generally, a small λ value of 0.01 leads to sub-optimal PSNR values, with Kodak08 showing the lowest PSNR of 13.42 dB. As λ increases to 0.1, the PSNR improves across all images, with Kodak01 achieving the highest PSNR of 17.64 dB. Further increasing λ to 0.2 results in continued improvements for some images, particularly Kodak12, which reaches a PSNR of 20.21 dB. Even a larger value of λ , such as 0.5, can lead to optimal performance in some cases, like Kodak01 and Kodak24, which present the highest PSNR of 18.17 dB and 16.71 dB.

IV. CONCLUSION

In this paper, we systematically investigated the vulnerabilities of INRs to weight perturbations for the first time. To address this issue, we formulate the robustness problem and derive a gradient-based loss to improve the model performance under noisy conditions. Extensive experiments on reconstruction tasks on multiple modalities, including natural image, CT, audio, and video, demonstrate that our method significantly enhances model robustness under various noise conditions by achieving gains of up to 7.5 dB in PSNR value compared to the baseline approach.

REFERENCES

[1] Ben Mildenhall, Pratul P Srinivasan, Matthew Tancik, et al., “NeRF: Representing Scenes as Neural Radiance Fields for View Synthesis,” in *ECCV*, 2020.

[2] Vincenzi Sitzmann, Julien NP Martel, Alexander W Bergman, et al., “Implicit Neural Representations with Periodic Activation Functions,” *NeurIPS*, 2020.

[3] Matthew Tancik, Pratul P Srinivasan, Ben Mildenhall, et al., “Fourier Features Let Networks Learn High Frequency Functions in Low Dimensional Domains,” in *NeurIPS*, 2020.

[4] Zeyuan Chen, Yinbo Chen, Jingwen Liu, Xingqian Xu, Vedit Goel, Zhenyang Wang, Humphrey Shi, and Xiaolong Wang, “VideoINR: Learning Video Implicit Neural Representation for Continuous Space-Time Super-Resolution,” in *Proceedings of the IEEE/CVF Conference on Computer Vision and Pattern Recognition*, 2022, pp. 2047–2057.

[5] Zhemin Li, Hongxia Wang, and Deyu Meng, “Regularize Implicit Neural Representation by Itself,” in *Proceedings of the IEEE/CVF Conference on Computer Vision and Pattern Recognition*, 2023, pp. 10280–10288.

[6] Jeong Joon Park, Peter Florence, Julian Straub, et al., “DeepSDF: Learning Continuous Signed Distance Functions for Shape Representation,” *CVPR*, 2019.

[7] Vincent Sitzmann, Michael Zollhoefer, and Gordon Wetzstein, “Scene Representation Networks: Continuous 3D-Structure-Aware Neural Scene Representations,” *NeurIPS*, 2019.

[8] Daniele Grattarola and Pierre Vandergheynst, “Generalised Implicit Neural Representations,” *Advances in Neural Information Processing Systems*, vol. 35, pp. 30446–30458, 2022.

[9] Sameera Ramasinghe and Simon Lucey, “Beyond Periodicity: Towards A Unifying Framework for Activations in Coordinate-MLPs,” in *European Conference on Computer Vision*. Springer, 2022, pp. 142–158.

[10] Junwon Seo, Sangyoon Lee, Kwang In Kim, and Jaeho Lee, “In Search of a Data Transformation That Accelerates Neural Field Training,” in *Proceedings of the IEEE/CVF Conference on Computer Vision and Pattern Recognition*, 2024, pp. 4830–4839.

[11] Chen Zhang, Steven Tin Sui Luo, Jason Chun Lok Li, Yik-Chung Wu, and Ngai Wong, “Nonparametric Teaching of Implicit Neural Representations,” in *Proceedings of the International Conference on Machine Learning*, 2024.

[12] Akhilan Boopathy, Tsui-Wei Weng, Pin-Yu Chen, Sijia Liu, and Luca Daniel, “Cnn-Cert: An Efficient Framework for Certifying Robustness of Convolutional Neural Networks,” in *Proceedings of the AAAI Conference on Artificial Intelligence*, 2019, vol. 33, pp. 3240–3247.

[13] Qi Zhang, Jingyu Xiao, Chunwei Tian, Jerry Chun-Wei Lin, and Shichao Zhang, “A robust deformed convolutional neural network (cnn) for image denoising,” *CAAI Transactions on Intelligence Technology*, vol. 8, no. 2, pp. 331–342, 2023.

[14] Nuri Benbarka, Timon Höfer, Andreas Zell, et al., “Seeing implicit neural representations as fourier series,” in *Proceedings of the IEEE/CVF Winter Conference on Applications of Computer Vision*, 2022, pp. 2041–2050.

[15] Shaohui Lin, Rongrong Ji, Chengqian Yan, Baochang Zhang, Liujuan Cao, Qixiang Ye, Feiyue Huang, and David Doermann, “Towards Optimal Structured CNN Pruning via Generative Adversarial Learning,” in *Proceedings of the IEEE/CVF conference on computer vision and pattern recognition*, 2019, pp. 2790–2799.

[16] Felix Sattler, Simon Wiedemann, Klaus-Robert Müller, and Wojciech Samek, “Robust and communication-efficient federated learning from non-iid data,” *IEEE transactions on neural networks and learning systems*, vol. 31, no. 9, pp. 3400–3413, 2019.

[17] Song Han, Huizi Mao, and William J Dally, “Deep compression: Compressing deep neural networks with pruning, trained quantization and huffman coding,” *arXiv preprint arXiv:1510.00149*, 2015.

[18] Mingzhe Chen, Deniz Gündüz, Kaibin Huang, Walid Saad, Mehdi Bennis, Aneta Vulgarakis Feljan, and H Vincent Poor, “Distributed learning in wireless networks: Recent progress and future challenges,” *IEEE Journal on Selected Areas in Communications*, vol. 39, no. 12, pp. 3579–3605, 2021.

[19] Yangxin Chen, “ReRAM: History, Status, and Future,” *IEEE Transactions on Electron Devices*, vol. 67, no. 4, pp. 1420–1433, 2020.

[20] Yaron Lipman, “Phase transitions, distance functions, and implicit neural representations,” *arXiv preprint arXiv:2106.07689*, 2021.

[21] Prasenjit Dey, Kaustuv Nag, Tandra Pal, and Nikhil R Pal, “Regularizing Multilayer Perceptron for Robustness,” *IEEE Transactions on Systems, Man, and Cybernetics: Systems*, vol. 48, no. 8, pp. 1255–1266, 2017.

[22] Vishwanath Saragadam, Daniel LeJeune, Jasper Tan, Guha Balakrishnan, Ashok Veeraraghavan, and Richard G Baraniuk, “WIRE: Wavelet Implicit Neural Representations,” in *Proceedings of the IEEE/CVF Conference on Computer Vision and Pattern Recognition*, 2023, pp. 18507–18516.

[23] Tianlong Chen, Zhenyu Zhang, Santosh Balachandra, Haoyu Ma, Zehao Wang, Zhenyang Wang, et al., “Sparsity Winning Twice: Better Robust Generalization from More Efficient Training,” in *International Conference on Learning Representations*, 2022.

[24] Ji Lin, Chuang Gan, and Song Han, “Defensive Quantization: When Efficiency Meets Robustness,” in *International Conference on Learning Representations*, 2020.

[25] Qi Xu, Junpeng Wang, Hao Geng, Song Chen, and Xiaoqing Wen, “Reliability-Driven Neuromorphic Computing Systems Design,” in *2021 Design, Automation & Test in Europe Conference & Exhibition (DATE)*, 2021, pp. 1586–1591.

[26] Francesca Pistilli, Diego Valsesia, Giulia Fracastoro, and Enrico Magli, “Signal Compression via Neural Implicit Representations,” in *ICASSP 2022-2022 IEEE International Conference on Acoustics, Speech and Signal Processing (ICASSP)*. IEEE, 2022, pp. 3733–3737.

[27] Amirali Molaei, Amirhossein Aminimehr, Armin Tavakoli, Amirhossein Kazerouni, Bobby Azad, Reza Azad, and Dorit Merhof, “Implicit Neural Representation in Medical Imaging: A Comparative Survey,” in *Proceedings of the IEEE/CVF International Conference on Computer Vision*, 2023, pp. 2381–2391.